

Thesis for the Degree of Master of Philosophy

**Motion Control of Welding Mobile
Manipulator Traveling on Irregular
Terrain**

by

Jae Sung Im

Department of Mechatronics Engineering

Graduate School

Pukyong National University

August 2005

Motion Control of Welding Mobile Manipulator Traveling on Irregular Terrain

**불규칙 지형을 이동하는 용접용 이동
매니퓰레이터와 자세 제어**



**Supervised by
Professor Sang Bong Kim**

Ja Sung Kim

**A thesis submitted in partial fulfillment of the requirements
for the degree of**

Master of Philosophy

**in the Department of Mechatronics Engineering, Graduate School
Pukyong National University**

August 2005

**Motion Control of Welding Mobile Manipulator Traveling on
Irregular Terrain**

A Dissertation

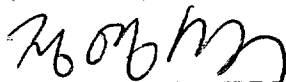
by

Jae Sung Im

Approved as to styles and content by:



YOUNG BOK KIM
(Chairman)



YOUNG SEOK JUNG
(Member)



SANG BONG KIM
(Member)

August 25, 2005

Acknowledgements

I have had the privilege of being with several exemplary professors and friends throughout my Master program; their exceptional help and support made this Master degree a pleasurable and exciting adventure.

First thanks must go to Professor Sang Bong Kim, my supervisor, for the priceless help and care throughout my program. I appreciate his spirit of enterprise, his vast knowledge in many areas, and his assistance in writing paper. I would like to thank the members of my thesis committee: Professor Young Bok Kim and Professor Young Seok Jung, for the helpful comments and suggestions.

I would like to thank Dr. Hak Kyeong Kim, Prof. Myung-Suk Lee, and Dr. Jin Ho Suh, who have a major role played in this study, both in their lectures and in life.

I am also grateful to all members of CIMEC Lab, for giving me a comfortable and active environment to achieve my study: Dr. Tan Tung Phan, Dr. Thien Phuc Tran, Mr. Tan Lam Chung, Mr. Manh Dung Ngo, Dr. Gun You Lee, Dr. Dong kyu Kim, Dr Tae Kyeong Yeu, Mr. Seung Mok Shin, Mr. Seok Yeol Kim, Mr Seung Wook Kim, Kim Mr. Soung Jea Park. Mr. Young Kyu Kim, Sang Chan Kim, Sung Chin Ma, Hak Cheol Lee, Joon Ho Jeong and others, for their great encouragement.

Last but not least, it is my pleasure to thank my parents and my younger brother for their endless encouragement.

Jae Sung Im

Contents

Acknowledgments

Abstract 1

Nomenclatures 3

1. Introduction 5

1.1 Motivation 5

1.2 Previous Research 6

1.3 Contributions of This Thesis 8

1.4 The Organization of This Thesis 8

2. System Modeling and Controller Design of a Mobile Manipulator 10

2.1 Configuration of the Mobile Manipulator 10

2.2 The Associated Coordinate Frames 11

2.3 Kinematic modeling for mobile platform 13

2.4 Traveling terrain model 14

2.5 Kinematic modeling for manipulator 15

2.6 Kinematic Equation of the Welding Torch Tip 18

2.7 Tracking errors 18

2.8 Kinematic Feedback Controller Design 20

3. Hardware Design and Implementation 25

3.1 Overall Control System 25

3.2 Sensor Design and Implementation 27

3.3	Motor Control	28
3.4	Microprocessor Control Design	32
4.	Simulation and Experimental Results	36
4.1	The Case of straight Line	37
4.2	The Case of Curve line	41
4.3	Experimental Results	45
5.	Conclusions and Future Work	47
5.1	Conclusions	47
5.2	The Future Work	48
5.2.1	Mobile Manipulator Modeling	48
5.2.2	Design of the controller	48
	References	50
	Publications and Conferences	53

Motion Control of Welding Mobile Manipulator Traveling on Irregular Terrain

Jae-Sung Im

**Department of Mechatronics Engineering, Graduate School
Pukyong National University**

Abstract

This thesis discusses about welding trajectory-tracking control method for a mobile manipulator traveling on irregular terrain. Its model of a kinematic mobile manipulator, estimation method of kinematic disturbance and kinematic feedback controller with the compensator are described.

It is well known, the mobile manipulator has infinite motion area, which brings several sophisticated advantages to the manipulator control. However, when the mobile manipulator travels on an unknown terrain, the mobile manipulator is subjected to the effect of the disturbance torques. Terrain irregularities exist even in structures such as the man-made floors of factories, buildings, and etc. Hence, in this paper, a model of a dynamic mobile manipulator traveling on irregular terrain is formulated with traveling states and constraint conditions. We evaluate disturbance torques derived by terrain during traveling on irregular terrain quantitatively based on the proposed model of a dynamic mobile manipulator. Relationships between changes in disturbance torques, changes in periods of terrain and changes in traveling speed are evaluated quantitatively by simulations. Then, the estimation of kinematic disturbance caused by irregular terrain is discussed. A compensation method of decreasing control errors caused by disturbances

due to terrain must be considered. The kinematic feedback controller with the compensator is proposed to improve the trajectory-tracking control performances.

In this thesis, Experiment is carried out with estimation of terrain shape using tilt sensors and robust control method with compensator of mobile manipulators traveling on irregular terrain. The mobile manipulator consists of a three-linked manipulator and a two-wheeled mobile platform. The vehicle is considered to move with a constant linear speed over an irregular ground-surface while the end-effector tracks a desired trajectory in a fixed reference frame. The experiment must be verified the effectiveness of the proposed controller. These results are shown to fit well by the simulation results.

Nomenclatures

Variables	Description	Units
$Oxyz$	world coordinate frame	
$Cx_my_mz_m$	moving frame	
$q_m^{(c)}$	joint angles of the manipulator in the moving frame	
$q_p^{(c)}$	configuration of the platform in the world frame	q
$p_i^{(c)}$	configuration of the mobile manipulator end effector position and orientation in the world frame	
$C(x_c, y_c)$	the coordinate of the platform's center point	
ϕ_c	heading angle of the platform	[rad]
r	radius of the wheels	[m]
h	distance from wheel to the symmetry axis	[m]
v_{xy}	straight velocity of the platform in x-y plane	[m/s]
ω_r	angular velocity of the right wheel	[rpm]
ω_l	angular velocity of the left wheel	[rpm]
r	radius of wheel	[m]
θ_i	link variables ($i = 1-4$)	[rad]
ω_i	angular velocity of the link ($i = 1-4$)	[rad/s]
q_E	configuration of the torch tip	

J	Jacobian matrix of the manipulator	
l_i	length of the link ($i = 1-5$)	[m]
ϕ_u	heading angle in the horizontal plane of the welding torch	[rad]
p_m	projection of the manipulator on x-y plane	[m]
ω_w	vertical angular velocity of the welding torch	[rad/s]
e_i	tracking errors ($i = 1-4$)	
$A(q)$	constraint matrix	
v_r	reference velocity of welding torch tip	[m/s]
v_z	z component velocity of the welding torch tip	[m/s]
V	Lyapunov function	
k_i	weight factors of the controller	
v_c	velocity control input	[m/s]

Subscripts

r	reference or desired value
w	welding or actual value
i	initial value

Chapter 1

Introduction

1.1 Motivation

Nowadays, the working condition in the industrial fields has been improved greatly. In the hazardous and harmful environments, the workers are substituted by the robots to perform the operations. Especially in welding field, the welders are substituted by the welding manipulators to perform the welding tasks.

Traditionally, the manipulators are fixed on the floor. Their workspaces are limited by the reachable abilities of their structures. In order to overcome this disadvantage, the manipulators that are movable are used for enlarging their workspaces. These manipulators are called the mobile manipulators^[20]. In this study, the structure of the mobile manipulator includes a three-linked manipulator plus a two-wheeled mobile platform. The mobile manipulator permits a wide application in industrial fields such as ship building industry, automobile industry, electronic assembling, and metal fabricating industry. It is also clear that moving and working at the same time can improve their working efficiency to a considerable extent. Though the researches on mobile manipulators have been presented in recent years, it is assumed that the traveling terrain is flat^[14].

However, since irregularities exist on surface over which the mobile manipulator is traveling, even in the case of man-made structures such as floors of factories and other buildings, and since it is difficult to measure the terrain shape precisely, a method that can compensate for disturbances (kinematic disturbances) due to the terrain shape is needed. And this is also the motivation of this

1.2 Previous Research

The previous works are concentrated on the following topics

- ***Motion control of a wheeled mobile robot***

The mobile platform is a subject of non-holonomic system. Assume that the wheels roll purely on a horizontal plane without slippage. The mobile platform robot used in this study has two independent driving wheels and one passive caster for balancing. Several researchers studied the wheeled mobile robot as a non-holonomic system. Kanayama *et al.*^[11] (1991) proposed a stable tracking control method for a non-holonomic mobile robot. The stability is guaranteed by Lyapunov function. Fierro and Lewis^[2] (1995) used the backstepping kinematic into dynamic method to control a non-holonomic mobile robot. Lee *et al.*^[3] (1999) proposed an adaptive control for a non-holonomic mobile robots using the computed torque method. Fukao *et al.*^[4] (2000) developed an adaptive tracking control method with the unknown parameters for the mobile robot. Bui *et al.*^[5] (2003) proposed a tracking control method with the tracking point outside the mobile robot.

- ***Motion control of a manipulator***

The control of a manipulator is an interesting area for research. In previous works, Craig *et al.*^[6] (1986) proposed an algorithm for estimating parameters on-line using an adaptive control law with the

computed torque method for the control of manipulators. Lloyd *et al.*^[7] (1993) proposed a singularity control method for the manipulator using closed-form kinematic solutions. Tang *et al.*^[8] (1998) proposed a decentralized robust control of a robot manipulator.

- ***Motion control of a mobile manipulator***

A manipulator mounted on a mobile platform will get a large workspace, but it also has many challenges. With regard to the kinematic aspect, the movement of the end effector is a compound movement of several coordinate frames at the same time. With regard to the dynamic aspect, the interaction between the manipulator and the mobile platform must be considered. With regard to the control aspect, whether the mobile manipulator is considered as two subsystems is also a problem that must be studied.

In previous works, Seraji^[9] (1995) developed a fully integrated kinematic model of the mobile manipulator rather than considering the mobile manipulator as two separate entities. Liu and Lewis^[10] (1990) developed a robust control for a mobile manipulator considering the mobile platform and the manipulator as two subsystems. Hootsmans and Dubowsky^[11] (1991) developed a control method to compensate the dynamic interactions between the mobile platform and the manipulator. Dong, Xu, and Wang^[12] (2000) studied a tracking control of a mobile manipulator with the effect of the interaction between two subsystems. Yamamoto^[13] (1994) made a complete study of the control and coordination of locomotion and manipulation of a wheeled mobile manipulator.

Furthermore, it can be applied in the hazardous environments such as waste

management, desolate exploration and even space operation. Especially, the mobile robots are extensively used in industry for resistance and arc-welding applications, in that industry, the pollution of the blazing light and smoke of arc make a necessary for automation the welding process.

1.3 Contributions of This Thesis

This thesis proposes and implements a Lyapunov-based nonlinear feedback control for a mobile manipulator to tracking welding line. As a result, the following contributions were made during this thesis work:

- (1) a kinematic model of a two-wheeled mobile robot was developed in Cartesian coordinates from which the system dynamics were derived;
- (2) a kinematic model of a manipulator was developed in Cartesian coordinates from which the system dynamics were derived;
- (3) a mechanical structure of mobile manipulator was made for the experiment;
- (4) feedback controller based on the Lyapunov function candidate are proposed, that is, full-state feedback controller;
- (5) a DSP-based microprocessor was implemented on the experimental mobile manipulator;
- (6) a configuration of sensor using two potentiometers and one tilt sensor is introduced to achieve the errors for the controllers;
- (7) the simulation in Matlab and the experiment results have been done to verify the two proposed controllers.

1.4 The Organization of This Thesis

This thesis consists of five chapters The content in each chapter are

summarized as follows:

▪ ***Chapter 1: Introduction***

The motivation, the related studies in literature, the contribution of this research, and the summary outline of contents of this thesis are presented.

▪ ***Chapter 2: Kinematic modeling and Controller design***

Present the system modeling of a welding wheeled mobile manipulator in kinematic model. The kinematic equations of a mobile manipulator are presented. These equations are based on the laws in mechanics. A controller is designed with full-state feedback. The former is designed using Lyapunov stability method.

▪ ***Chapter 3: Hardware Design and Implementation***

The overall control system is described. The control system based DSP is introduced. Also, a configuration of sensor sensing the errors of distance and angle from the mobile manipulator to the weld line is proposed.

▪ ***Chapter 4: Simulations and Experimental Results***

Simulation and experimental results for the mobile manipulator to tracking straight line and curve line are given to show the effectiveness of the proposed controller

▪ ***Chapter 5: Conclusions and Future Work***

Summary this thesis results and the future work.

Chapter 2

System Modeling and Controller Design of a Mobile Manipulator

In this Chapter, the kinematic equations of the manipulator and the mobile platform are investigated^[17]. These equations will be used to establish the controller for the mobile manipulator in subsection 2.8.

2.1 Configuration of the Mobile Manipulator

The mobile manipulator that be used in this thesis is the combination of a mobile platform robot and the multilink manipulator as shown in Fig. 1. The mobile platform robot is a two wheels driving platform of kind and the manipulator is a 5 d.o.f. manipulator.

We must pay attention to the constraint that the direction of the torch must lay on the tangent plane of welding path at the welding point. Furthermore, the direction of the torch must also incline 45 degrees beside the plane of welding path.

According to the above conditions, in the configuration of manipulator, we fix the torch direction on the tilt of 45 degrees beside the link direction of link 4-th. And the link direction of link 4-th (and link-3th too) always be kept in the perpendicular direction of the welding path plane.

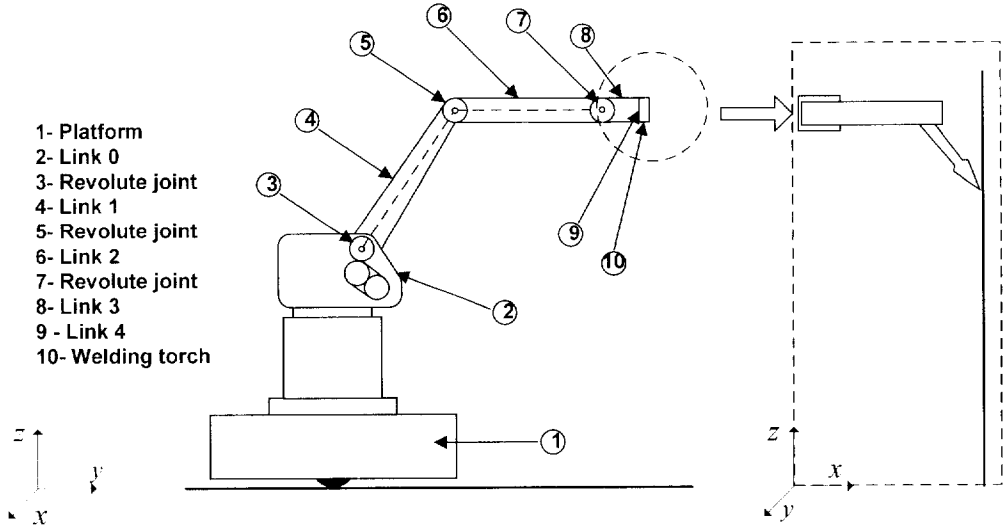


Fig. 2-1. Mobile manipulator configuration.

2.2 The Associated Coordinate Frames

Two coordinate frames are set up for investigating the system model (see Fig. 2.4 for more detail). Together with both of coordinate frame, for easy reference, all the definitions of the state variables for mobile manipulator, mobile platform and the manipulator are listed as the following:

- O_{xyz} : world coordinate frame, it is also the inertia coordinate frame.
- $C_{x_m y_m z_m}$: moving frame, it is the frame attached on the mobile manipulator.
- $q_m^c = \{d_0, \theta_1, \theta_2, \theta_3, \theta_4\}^T$: configuration of the manipulator in the moving frame.
- $q_p^O = \{x_c, y_c, \phi\}^T$: configuration of the platform in the world frame.

- $q = \{x_c, y_c, \phi, \theta_1, \theta_2, \theta_3, \theta_4\}^T$: configuration of the mobile manipulator
- $p_i^O = \{x_w, y_w, z_w, \phi, \psi, \theta\}^T$: end effector position and orientation in the world frame.

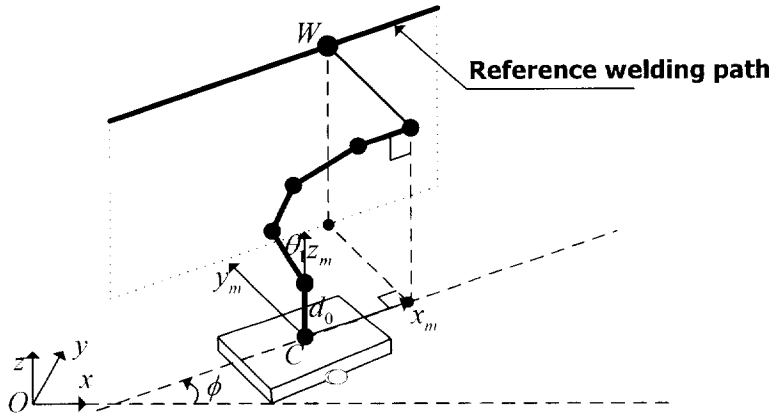


Fig. 2-2. Coordinate frames and state variables of the mobile manipulator.

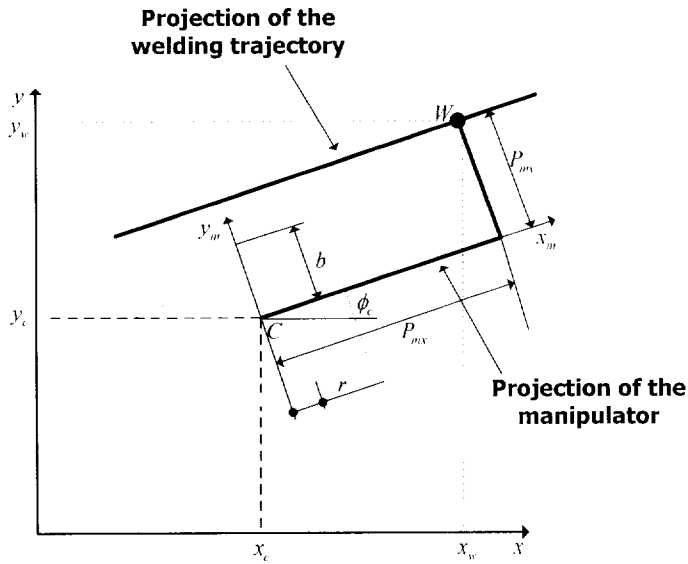


Fig. 2-3 Kinematic relationship of the mobile platform.

2.3 Kinematic modeling for mobile platform

The kinematic equation of the platform can be described as the following (see in figure 2-3):

$$\begin{bmatrix} \dot{x}_c \\ \dot{y}_c \\ \dot{\phi} \\ \dot{\theta}_r \\ \dot{\theta}_l \end{bmatrix} = \begin{bmatrix} \cos \phi & 0 \\ \sin \phi & 0 \\ 0 & 1 \\ 1/r & b/r \\ 1/r & -b/r \end{bmatrix} \begin{bmatrix} v_{xy} \\ \omega_\phi \end{bmatrix} \quad (2.1)$$

where $\mathbf{q}_p = [x_c \ y_c \ \phi \ \theta_r \ \theta_l]^T$ is the generalized coordinate of the mobile platform, for more detail, $C(x_c, y_c, 0)$ is the coordinate of the platform's center point, and ϕ is the heading angle of the platform; ω_ϕ is the angular velocity of the platform at its center point; v_{xy} is the straight velocity of the platform in x-y plane; r, b are radius of wheel and the distance from wheel to the symmetry axis, respectively; $\dot{\theta}_r, \dot{\theta}_l$ are the angular velocity of the mobile platform's wheels.

It is assumed that the wheels of mobile platform do not slip. So, the velocity of C must be kept in the direction of the axis of symmetry and the wheels must purely roll.

The constraints are expressed as follows:

$$\mathbf{A}(\mathbf{q}_p)\dot{\mathbf{q}}_p = 0 \quad (2.2)$$

or for this case:
$$\begin{bmatrix} -\sin \phi & \cos \phi & 0 & 0 & 0 \\ \cos \phi & \sin \phi & b & -r & 0 \\ \cos \phi & \sin \phi & -b & 0 & -r \end{bmatrix} \begin{bmatrix} \dot{x}_c \\ \dot{y}_c \\ \dot{\phi} \\ \dot{\theta}_r \\ \dot{\theta}_l \end{bmatrix} = 0$$

2.4 Traveling terrain model

The modeled terrain shape for the mobile manipulator shown in Fig. 2-4 is described by the sum of trigonometric functions having various amplitudes and periods. The shape can be expressed by a Fourier series and is defined by the following function $f(x)$.

$$f(x) = \frac{a_0}{L} + \frac{2}{L} \sum_{s=1}^{\infty} (a_s \cos c_s x + b_s \sin c_s x)$$

$$a_s = \int_0^L f(x) \cos c_s x dx$$

$$b_s = \int_0^L f(x) \sin c_s x dx, \quad c_s = \frac{2s\pi}{L}$$
(2.3)

The length of $d(t)$ is estimated by the following function.

$$d(x) = d(x-1) + v_c \sin \theta_1 dx$$
(2.4)

The shape looked just like plane mechanism with two links. Therefore, we can assume that the terrain shape is virtual manipulator with two links as shown in Fig. 2-4.

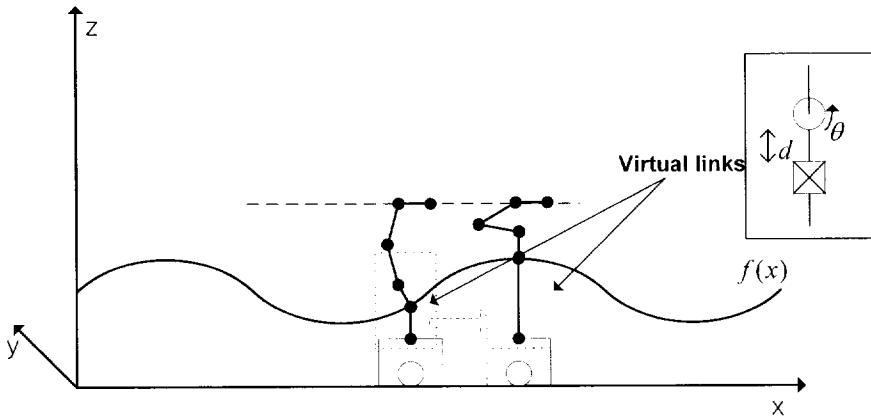


Fig. 2-4. Traveling Terrain.

2.5 Kinematic modeling for manipulator

A five-link manipulator is shown in Fig. 2- 5 where l_1, l_2, l_3, l_4 and l_5 are the fixed and known link length parameters and d_0 and θ_1 are relation of the terrain shape.

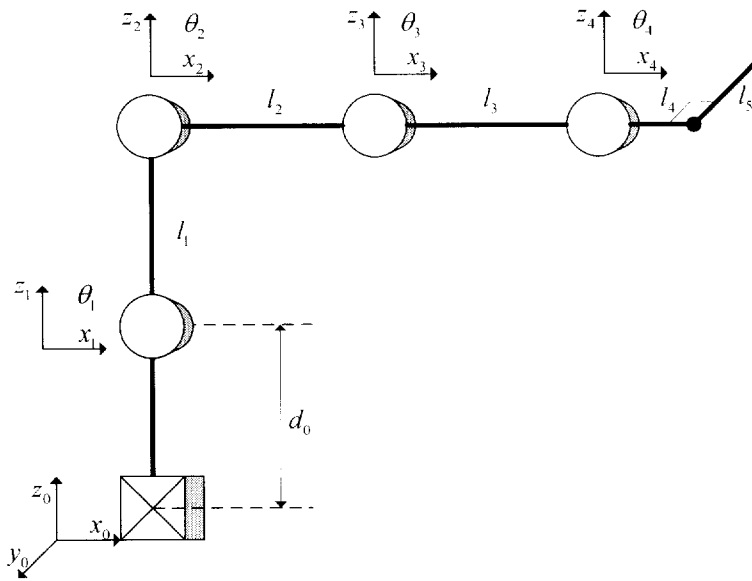


Fig. 2-5. Modeling and coordinate of the manipulator.

The joint vector is

$$q_m = [d_0 \quad \theta_1 \quad \theta_2 \quad \theta_3 \quad \theta_4]. \quad (2.5)$$

By inspection, the A matrices are found to be

$$\begin{aligned}
A_0 &= \begin{bmatrix} 1 & 0 & 0 & 0 \\ 0 & 1 & 0 & 0 \\ 0 & 0 & 1 & d_0 \\ 0 & 0 & 0 & 1 \end{bmatrix}, & A_1 &= \begin{bmatrix} \cos \theta_1 & 0 & \sin \theta_1 & l_1 \sin \theta_1 \\ 0 & 1 & 0 & 0 \\ -\sin \theta_1 & 0 & \cos \theta_1 & l_1 \cos \theta_1 \\ 0 & 0 & 0 & 1 \end{bmatrix}, \\
A_2 &= \begin{bmatrix} \cos \theta_2 & 0 & \sin \theta_2 & l_2 \sin \theta_2 \\ 0 & 1 & 0 & 0 \\ -\sin \theta_2 & 0 & \cos \theta_2 & l_2 \cos \theta_2 \\ 0 & 0 & 0 & 1 \end{bmatrix}, & A_3 &= \begin{bmatrix} \cos \theta_3 & 0 & \sin \theta_3 & l_3 \sin \theta_3 \\ 0 & 1 & 0 & 0 \\ -\sin \theta_3 & 0 & \cos \theta_3 & l_3 \cos \theta_3 \\ 0 & 0 & 0 & 1 \end{bmatrix}, \\
A_4 &= \begin{bmatrix} \cos \theta_4 & 0 & \sin \theta_4 & l_4 \sin \theta_4 \\ 0 & 1 & 0 & 0 \\ -\sin \theta_4 & 0 & \cos \theta_4 & l_4 \cos \theta_4 \\ 0 & 0 & 0 & 1 \end{bmatrix}, & A_5 &= \begin{bmatrix} 1 & 0 & 0 & 0 \\ 0 & 1 & 0 & l_5 \\ 0 & 0 & 1 & 0 \\ 0 & 0 & 0 & 1 \end{bmatrix}
\end{aligned}$$

The T matrix is

$$\begin{aligned}
T &= A_0 A_1 A_2 A_3 A_4 A_5 \\
&= \begin{bmatrix} C_{1234} & 0 & S_{1234} & l_4 + l_3 S_{123} + l_2 S_{12} + l_1 S_1 \\ 0 & 1 & 0 & l_5 \\ -S_{1234} & 0 & C_{1234} & l_3 C_{123} + l_2 C_{12} + l_1 C_1 + d_0 \\ 0 & 0 & 0 & 1 \end{bmatrix} \tag{2.6}
\end{aligned}$$

Where, $C_{12\cdots i}$ is the abbreviation of $\cos(\theta_1 + \theta_2 + \cdots \theta_i)$ and $S_{12\cdots i}$ is the abbreviation of $\sin(\theta_1 + \theta_2 + \cdots \theta_i)$

In operation, the manipulator is considered as x-y plane mechanism with five links (adding links of terrain shape) as shown in Fig 2-6.

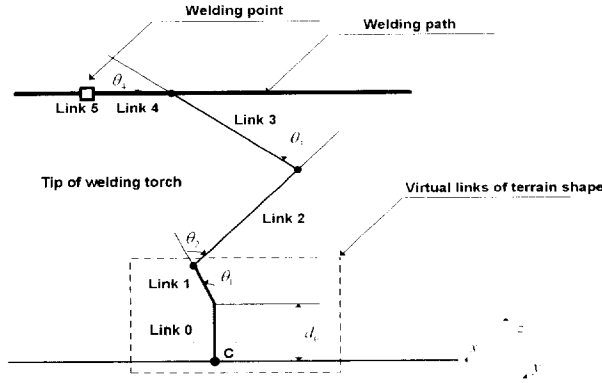


Fig. 2-6 Manipulator motion in welding process

In addition, on welding process, to retain the correct direction of torch beside the welding path, the fourth link is always fixed on horizontal. That is to say:

$$\begin{aligned}\theta_1 + \theta_2 + \theta_3 + \theta_4 &= \frac{\pi}{2} \\ w_1 + w_2 + w_3 + w_4 &= 0\end{aligned}\quad (2.7)$$

Therefore, the position in base coordinates of the end of the manipulator, that is, the origin of frame 0, is

$$\mathbf{P} = \begin{bmatrix} x_p \\ y_p \\ z_p \end{bmatrix} = \begin{bmatrix} l_4 + l_3 S_{123} + l_2 S_{12} + l_1 S_1 \\ l_5 \\ l_3 C_{123} + l_2 C_{12} + l_1 C_1 + d_0 \end{bmatrix} \quad (2.8)$$

$$\theta_1 = \frac{\pi}{2} - \theta_2 - \theta_3 - \theta_4 \quad (2.9)$$

$$\mathbf{P} = \begin{bmatrix} x_p \\ y_p \\ z_p \end{bmatrix} = \begin{bmatrix} l_4 + l_3 C_4 + l_2 C_{34} + l_1 C_{234} \\ l_5 \\ l_3 S_4 + l_2 S_{34} + l_1 S_{234} + d_0 \end{bmatrix} \quad (2.10)$$

Now, we establish the equation describing the coordinate of the welding point, $\mathbf{W}(x_w, y_w, z_w)$, by means of coordinate of platform's center and the link variables of manipulator. Of course, we also remark that the heading angle of the platform

is constantly 90° , that is to say, the platform always moves on the path that is parallel with the plane of reference welding path, and so $y_w = \text{constant}$:

$$\begin{aligned}x_w &= x_c + x_p \\y_w &= y_c - y_p \\z_w &= z_p\end{aligned}\tag{2.11}$$

The kinematic equation of the manipulator can be described as the following:

$$\begin{bmatrix} \dot{x}_p \\ \dot{z}_p - \dot{d}_0 \\ w_p \end{bmatrix} = \begin{bmatrix} -l_1 S_{234} & -(l_1 S_{234} + l_2 S_{34}) & -(l_1 S_{234} + l_2 S_{34} + l_3 S_4) \\ l_1 C_{234} & l_1 C_{234} + l_2 C_{34} & l_3 C_4 + l_2 C_{34} + l_1 C_{234} \\ 1 & 1 & 1 \end{bmatrix} \begin{bmatrix} \dot{\theta}_2 \\ \dot{\theta}_3 \\ \dot{\theta}_4 \end{bmatrix}\tag{2.12}$$

The inverse kinematic equation is defined as (referring Eq. 2.7):

$$\begin{bmatrix} w_2 \\ w_3 \\ w_4 \end{bmatrix} = \begin{bmatrix} \dot{\theta}_2 \\ \dot{\theta}_3 \\ \dot{\theta}_4 \end{bmatrix} = \begin{bmatrix} \frac{\cos_4}{l_2 \sin_3} & \frac{\sin_4}{l_2 \sin_3} & \frac{l_1 \sin_{23} + l_2 \sin_3}{l_2 \sin_3} \\ \frac{-l_2 \cos_{34} - l_3 \cos_4}{l_2 l_3 \sin_3} & \frac{-l_2 \sin_{34} - l_3 \sin_4}{l_2 l_3 \sin_3} & \frac{-l_1 (l_2 \sin_2 + l_3 \sin_{23})}{l_2 l_3 \sin_3} \\ \frac{\cos_{34}}{l_3 \sin_3} & \frac{\sin_{34}}{l_3 \sin_3} & \frac{l_1 \sin_2}{l_3 \sin_3} \end{bmatrix} \begin{bmatrix} \dot{x}_p \\ \dot{z}_p - \dot{d}_0 \\ w_p \end{bmatrix}\tag{2.13}$$

2.6 Kinematic Equation of the Welding Torch Tip

The relationship between the welding point W and the center of the mobile platform C can be expressed as following (referring Eq. 2.11):

$$\begin{bmatrix} x_w \\ y_w \\ z_w \\ \phi_w \end{bmatrix} = \begin{bmatrix} x_c + P_{mx} \cos \phi_c - P_{my} \sin \phi_c \\ y_c + P_{mx} \sin \phi_c + P_{my} \cos \phi_c \\ l_3 S_4 + l_2 S_{34} + l_1 S_{234} + d_0 \\ \phi_c \end{bmatrix}\tag{2.14}$$

Where P_{mx}, P_{my} is the distance from the projection of the manipulator torch tip on the x-y plane to the center C of platform, ϕ_w is the heading angle in the

horizontal plane of the welding torch and ϕ_c is the heading angle of the mobile platform.

Combining the derivative of (2.14) and the angular velocity of the torch yields the kinematic equation for the welding torch tip as follows:

$$\begin{bmatrix} \dot{x}_w \\ \dot{y}_w \\ \dot{z}_w \\ \dot{\phi}_w \end{bmatrix} = \begin{bmatrix} \cos \phi_c & -(P_{mx} \sin \phi_c + P_{my} \cos \phi_c) & \cos \phi_c & 0 \\ \sin \phi_c & P_{mx} \cos \phi_c - P_{my} \sin \phi_c & \sin \phi_c & 0 \\ 0 & 0 & 0 & 1 \\ 0 & 1 & 0 & 0 \end{bmatrix} \begin{bmatrix} V_c \\ w_c \\ V_{mx} \\ V_{mz} \end{bmatrix} \quad (2.15)$$

2.7 Tracking errors

Vector $[e_1 \ e_2 \ e_3 \ e_4]^T$ is denoted as the vector of the tracking error that is the difference between the welding point V and the reference point R (see Fig. 2-7, 2-8). This vector is expressed as:

$$\begin{bmatrix} e_1 \\ e_2 \\ e_3 \\ e_4 \end{bmatrix} = \begin{bmatrix} \cos \phi_w & \sin \phi_w & 0 & 0 \\ -\sin \phi_w & \cos \phi_w & 0 & 0 \\ 0 & 0 & 1 & 0 \\ 0 & 0 & 0 & 1 \end{bmatrix} \begin{bmatrix} x_r - x_w \\ y_r - y_w \\ z_r - z_w \\ \phi_r - \phi_w \end{bmatrix} \quad (2.16)$$

Where the subscript r and w imply reference and welding (or desired and actual), respectively.

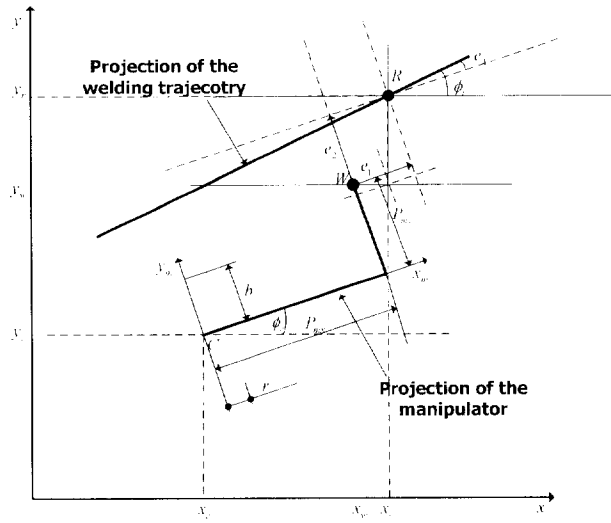


Fig. 2-7 Tracking errors description(e_1, e_2, e_4)

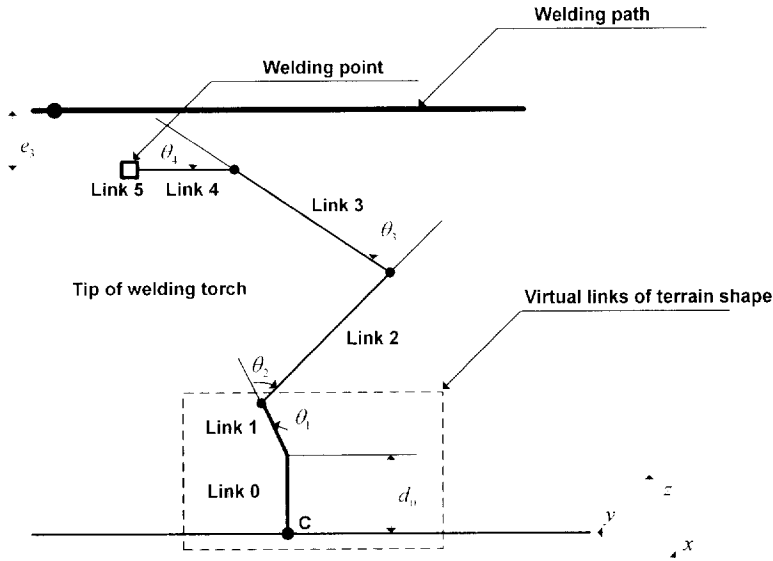


Fig. 2-8 Tracking errors description(e_3)

2.8 Kinematic Feedback Controller Design

As mentioned the sub-section 2-7, the tracking errors of the system are assumed to be bounded and they can be expressed as the following (see Fig. 2.7,

2.8 for more detail):

$$\begin{bmatrix} e_1 \\ e_2 \\ e_3 \\ e_4 \end{bmatrix} = \begin{bmatrix} \cos \phi_w & \sin \phi_w & 0 & 0 \\ -\sin \phi_w & \cos \phi_w & 0 & 0 \\ 0 & 0 & 1 & 0 \\ 0 & 0 & 0 & 1 \end{bmatrix} \begin{bmatrix} x_r - x_w \\ y_r - y_w \\ z_r - z_w \\ \phi_r - \phi_w \end{bmatrix} \quad (2.17)$$

Herein, tracking is concerned as the objective so a controller should be found out so that it can make the mobile manipulator obtaining $e_i \rightarrow 0$ with respect to $t \rightarrow \infty$. In the other word, the welding point W becomes to coincide with its reference point R , or the actual configuration concurs with the desired configuration of the end effector.

Easily, the derivative form of the errors in Eq. (2.17) can be established as the following:

$$\begin{bmatrix} \dot{e}_1 \\ \dot{e}_2 \\ \dot{e}_3 \\ \dot{e}_4 \end{bmatrix} = \begin{bmatrix} V_r \cos e_4 \\ V_r \sin e_4 \\ \dot{d}_0 \\ w_r \end{bmatrix} + \begin{bmatrix} -1 & e_2 + P_{my} & -1 & 0 \\ 0 & -(e_1 + P_{mx}) & 0 & 0 \\ 0 & 0 & 0 & -1 \\ 0 & -1 & 0 & 0 \end{bmatrix} \begin{bmatrix} V_c \\ w_c \\ V_{xm} \\ V_{zm} \end{bmatrix} \quad (2.18)$$

where, v_r is the reference velocity in the welding trajectory, it is assumed as a bounded and constant value; v_c is the x-y component velocity of the mobile platform; v_{zm} is the z component velocity of the end effector of the manipulator; v_{xm} is the x component velocity of the end effector of the manipulator; ω_ϕ is the derivative form of the heading angle ϕ , respectively; and p_m is the projection of the manipulator on x-y plane.

A candidate Lyapunov function is proposed as the following: (it is also chosen so that to be positive definite function)

$$V = \frac{1}{2}e_1^2 + \frac{1}{2}e_2^2 + \frac{1}{2}e_3^2 + \frac{1 - \cos e_4}{k_2} + \frac{1}{2k_5}P_{mx}^2 \quad (2.19)$$

The derivative form of (2.19) can be expressed as:

$$\begin{aligned}
\dot{V} &= e_1 \dot{e}_1 + e_2 \dot{e}_2 + e_3 \dot{e}_3 + \frac{\sin e_4}{k_2} \dot{e}_4 \\
&= e_1 (v_r \cos e_4 - v_c + P_{mY} \omega_c - v_{xm}) + \\
&\quad e_2 (v_r \sin e_4 - P_{mX} \omega_c) + e_3 (\dot{d}_0 - v_{zm}) + \\
&\quad \frac{\sin e_4}{k_2} (\omega_r - \omega_c) + \frac{P_{mX}}{k_5} \dot{P}_{mX}
\end{aligned} \tag{2.20}$$

The control variables are chosen as the following:

$$\begin{cases} v_c = v_r \cos e_4 + w_c P_{mY} - v_{xm} + k_1 e_1 \\ v_{zm} = \dot{d}_0 + k_3 e_3 \\ w_c = w_r + k_4 \sin e_4 + k_2 e_2 v_r \\ \dot{P}_{mX} = k_5 w_c e_2 \end{cases} \tag{2.21}$$

where k_1, k_2, k_3, k_4, k_5 are positive values.

Substituting Eq. (2.21) into Eq.(2.20), eliminating the similar terms for simplifying, the brief form of \dot{V} can be expressed as the following:

$$\dot{V} = -k_1 e_1^2 - k_3 e_3^2 - \frac{k_4}{k_2} \sin^2 e_4 \leq 0 \tag{2.22}$$

For proving $e_i \rightarrow 0$ as $t \rightarrow \infty$, the Barbalat's lemma is used in the following procedure. As for first condition of the lemma, referring Eq. (2.17), because e_i are bounded, the chosen Lyapunov function has a finite limit as $t \rightarrow \infty$ ^{[18][19]}. As for second condition of the lemma, the value of the derivative of \dot{V} is calculated as below:

$$\frac{d\dot{V}}{dt} = -2k_1 e_1 \dot{e}_1 - 2k_3 e_3 \dot{e}_3 - \frac{2k_4}{k_2} \dot{e}_4 \sin e_4 \cos e_4 \tag{2.23}$$

Obviously, because \dot{e}_i are bounded, the derivative of \dot{V} is bounded too. Therefore \dot{V} satisfies the sufficient condition of a uniformly continuous function. According to two above-mentioned conditions, by Barbalat's lemma, the result is obtained as $\lim_{t \rightarrow \infty} \dot{V} = 0$.

Now, Eq. (2.23) can be re-written as follows:

$$0 = -k_1 e_1^2 - k_3 e_3^2 - \frac{k_4}{k_2} \sin^2 e_4 \quad (2.24)$$

Eq. (2.24) implies that $\lim_{t \rightarrow 0} [e_1 \ e_2 \ e_3 \ e_4]^T = 0$. As a result of $e_4 = 0$, the welding heading angle and reference heading angle of mobile platform coincide, that is to say, $\omega_c = \omega_r$. Referring Eq. (2.19), in the third row, when two previous conditions occur, the result is $\lim_{t \rightarrow \infty} e_2 = 0$.

After everything mentioned above, a conclusion can be inferred: the equilibrium point $e_i = 0$ is uniformly asymptotically stable.

Based on the kinematic relationships in section 2-3, 2-5, the control input of system can be expressed as the following:

$$\begin{bmatrix} w_r \\ w_l \\ w_2 \\ w_3 \\ w_4 \end{bmatrix} = \begin{bmatrix} \frac{1}{r} & 0 & \frac{b}{r} \\ \frac{1}{r} & 0 & -\frac{b}{r} \\ 0 & \frac{\sin_4}{l_2 \sin_3} & 0 \\ 0 & \frac{-l_2 \sin_{34} - l_3 \sin_4}{l_2 l_3 \sin_3} & 0 \\ 0 & \frac{\sin_{34}}{l_3 \sin_3} & 0 \end{bmatrix} \begin{bmatrix} v_{xv} \\ v_{zm} \\ \omega_c \end{bmatrix} \text{ and } \omega_1 = -\omega_2 - \omega_3 - \omega_4 \quad (2.25)$$

The development of the control system can be illustrated by the following block diagram:

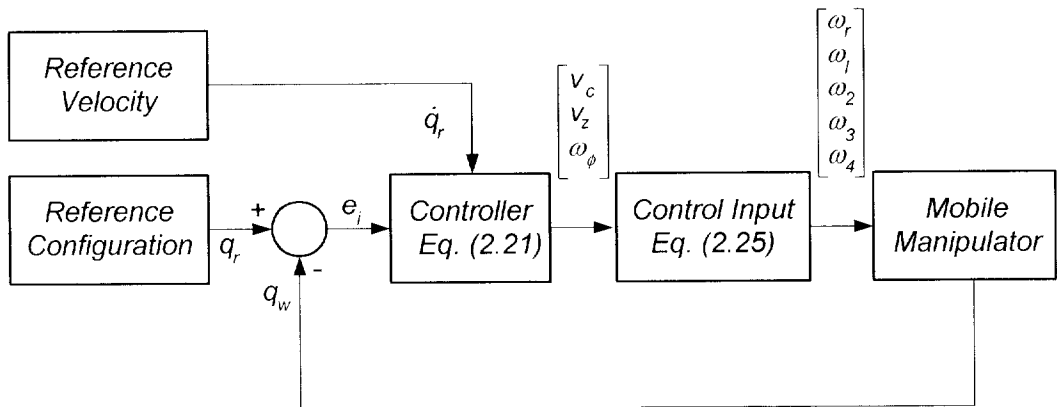


Fig. 2-9 Block diagram of the kinematic feedback control for mobile manipulator

Chapter 3

Hardware Design and Implementation

3.1 Overall Control System

For the control system, a DSP-based controller was developed. The configuration diagram of the total control system is shown in Fig. 3-1. In the diagram, the microprocessor using TMS320LF2407 is integrated into on module as servo controllers for five motors of the two wheels, and three links. The motors are driven via LMD18200 Dual Full-bridge Drivers. This module implements Lyapunov-based velocity control using feedback from an optical encoder attached to the rear motors. Also, the microprocessor receives the signal from sensors, render the control law, and send velocity information to the servo modules and the servo module are responsible for reaching and maintaining that speed. With the modular structure, the control system can manage a control law with a sampling time of 10ms, even 5ms in some critical applications. In addition, the eight A/D channel on microprocessor are used to receive signals from one tilt sensor, the sensor of two potentiometers: linear and angular potentiometers for errors measurement. The implementation of the control system is shown in Fig. 3-2.

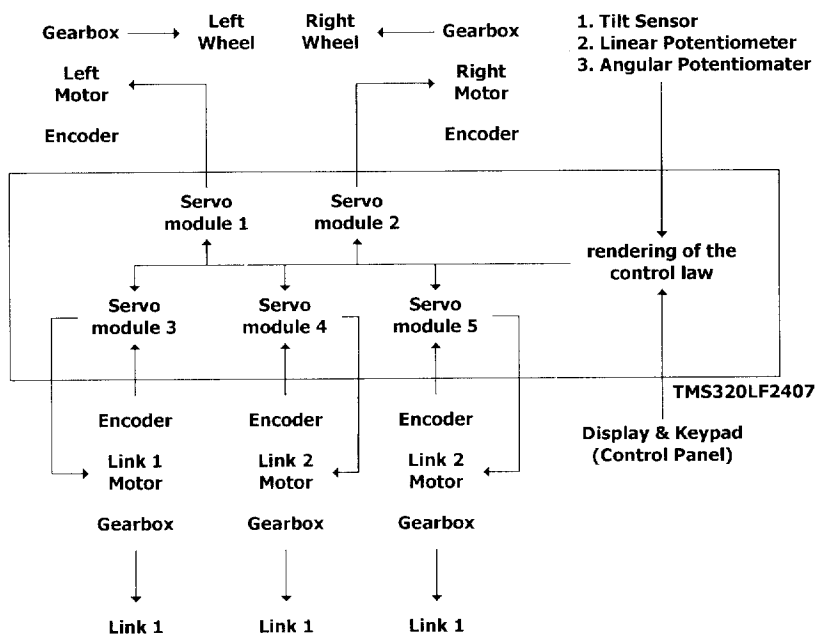


Fig. 3-1 Configuration of the control system

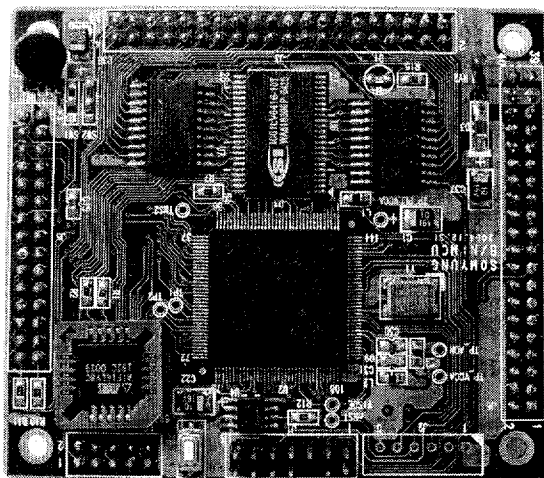


Fig. 3-2 DSP-based control system

3.2 Sensor Design and Implementation

As mentioned, the mobile manipulator itself must be located its position relative to the reference path; that is to say, the tracking errors must be measured, and the controllers are derived based on those errors. There are some methods for measuring these errors depending on the type of sensor to be used. In the other hand, as there is some restricted measurement scheme is proposed, and the sensor is specially designed using potentiometers to get the errors e_1, e_2 and e_4 for the controller (2.20). In Fig. 3-3, two rollers are placed at points O_1 and O_2 , and the distance between them, O_1O_2 , is chosen according to the curve radius of the reference path at contact point $R(x_r, y_r, \phi_r)$. The roller diameters are chosen small enough to overcome the friction force.

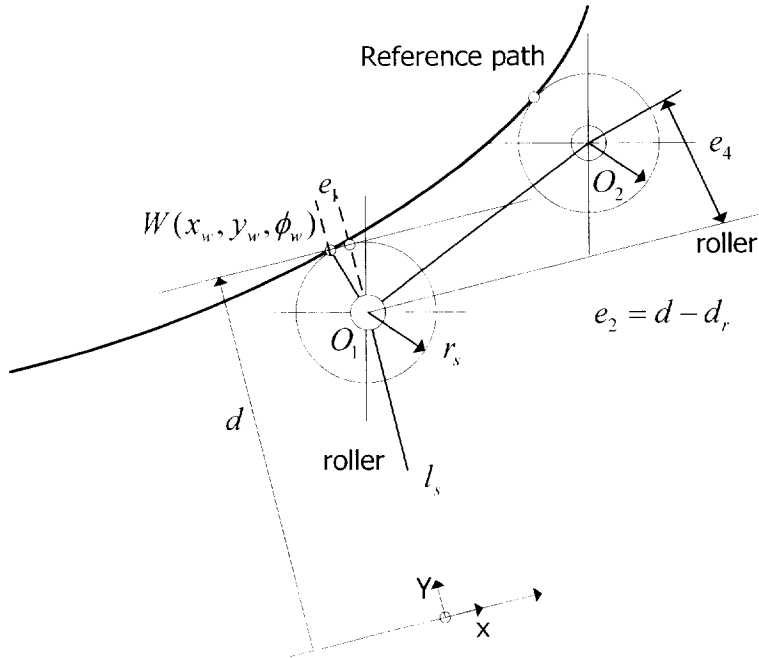


Fig. 3-3 Scheme and implementation for measuring the errors

3.3 Motor Control

To control the speed of a DC motor we need a variable voltage DC power source. If be powered on by a switch, the motor do not respond immediately, that is, it takes a small time to reach full speed; the motor will start to slow down; as the result, if we switch the power on and off quickly enough, the motor will run at some speed part way between zero and full speed. It is exactly the principle that a PWM controller does: it switches the motor on in a series of pulses. To control the motor speed, the width of the pulses varies – Pulse Width Modulation.

To perform indirect closed loop velocity control, an optical encoder is utilized to measure the speed of the wheel and links (Fig. 3-4). Incremental encoders typically consist of a light source, a rotating pattern disc, a stationary detector, and processing electronics to convert the analog detector signal to a digital output (Fig. 3-5). This type of encoder has two channels, which output digital square waves proportional to the number of windows on the optical code disc. The output of the encoder is a square wave whose frequency is proportional to the angular velocity of the rear wheels. The typical wave form of output is presented in Fig. 3-6.

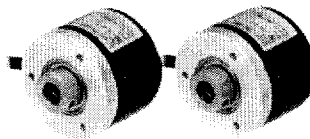


Fig. 3.4 Typical incremental encoder

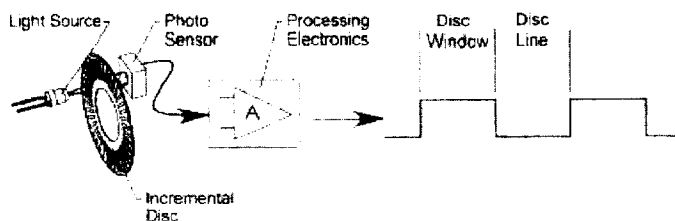


Fig. 3-5 Components of an incremental encoder

Incremental square waves are counted by a controller to determine wheel position, velocity and acceleration. Additionally, by observing the phase sequence between the two digital output channels, a controller can determine the direction of wheel rotation.

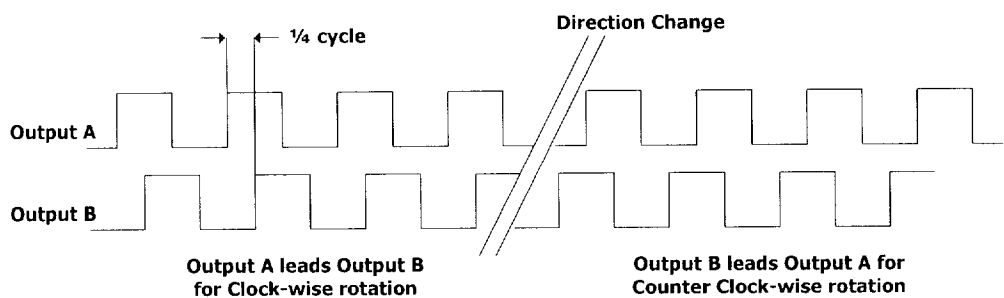


Fig. 3-6 Output wave form of an encoder

A third channel with a one per rotation signal is often found on incremental encoders and is commonly called the index or reference pulse (Fig.3-7). This signal is typically used to mark a particular location in a system's rotation that equates to a known mechanical location often called a home position. The drawback to an incremental encoder in a control system is if the controller's counter should happen to lose power or miscount, the system must be cycled back to a known location, such as an index location, before restarting. Often times an absolute encoder is used instead of an incremental encoder in order to overcome the cost, inconvenience and potential frequency of a home cycle restart sequence. In this application, the index pulse is not to be used.

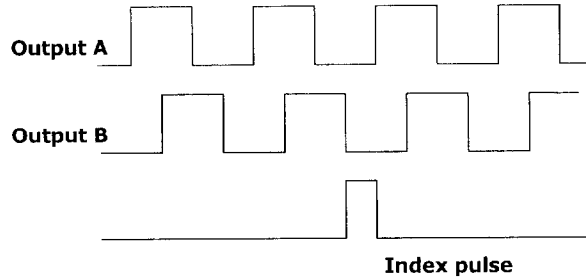


Fig. 3-7 Incremental encoder: the two channels and index pulse

Motor controller performs a closed loop velocity control. The angular velocity (rpm) is calculated as the following equation:

$$S = \frac{\text{Counts} / P}{T} \times 60 \quad (3.2)$$

where.

S : angular velocity of motor, *rpm*

Counts : number of pulses counted during the sampling time of T

P : number of pulses per revolution of encoder, *pulse*

T : sampling time, *s*

The motor driver using pin RC2 for PWM generation and pin RC1 for capture pulse from encoder. Motor controller counts the rising edges for a period of time to produce real angular velocity of the wheel. If the real velocity lowers than the desired angular velocity, the velocity must be increased. The behavior for the motor to speed up and down is performed using Lyapunov function.

▪ *Velocity control using Lyapunov function*

The configuration for the experiment is shown in Fig. 3-8.

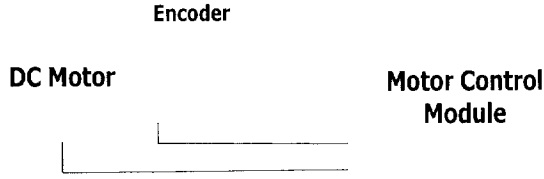


Fig. 3-8 Experimental configuration for velocity control

First, the following relationship has to be set up:

$$\omega = KV \quad (3.3)$$

Where

ω : angular velocity of the motor.

K : characteristic constant of the motor, and it is achieved by experiment.

V : average voltage applied to the motor.

The experiment gives $K = 274$ for this case

$$\dot{\omega} = Ku \quad \text{where } u = \dot{V} \quad (3.4)$$

Let $\varepsilon = \omega - \omega_r$

$$\begin{aligned} \dot{\varepsilon} &= \dot{\omega} - \dot{\omega}_r \\ &= Ku - \dot{\omega}_r \end{aligned} \quad (3.5)$$

If we choose

$$Ku - \dot{\omega}_r = -K_1 \varepsilon \quad (3.6)$$

then

$$\dot{\varepsilon} = -K_1 \varepsilon \leq 0 \quad (3.7)$$

and the velocity control is asymptotically stable

Form (3.4) we have

$$\dot{V} = u = \frac{-K_1 \varepsilon - \dot{\omega}_r}{K} \quad (3.8)$$

The duty of the PWM signal can be derived from V , the voltage applied to the motor. The simulation has done with $K_1 = 30$; and it can be seen that the motor's velocity can reach to the critical reference velocity with stable after about 0.18 seconds.

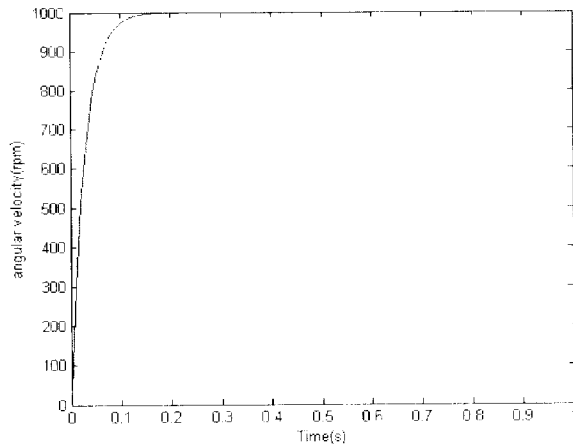


Fig. 3-9 Velocity response with $k_1 = 30$

3.4 Microprocessor Control Design

The TMS320LF2407 is a 144-pin, high performance static CMOS processor from TI(Texas Instruments). The main specifications of it are summarized as following:

- 33-ns Instruction Cycle Time (30 MHz)
- On-Chip memory:
 - 2.5K Words x 16 Bits of Flash EEPROM
 - Data/Program RAM
(544 Words of Dual-Access (DARAM)
2K Words of Single-Access (SARAM))
- Two Event-Manager (EV) Modules (A and B)
EVA and EVB Each Include:
 - Two 16-Bit General-Purpose Timers
 - Eight 16-Bit Pulse-Width Modulation
(PWM) Channels Which Enable:
 - Three-Phase Inverter Control

- Centered or Edge Alignment of PWM Channels
- Emergency PWM Channel Shutdown With External PDPINT Pin
- Three Capture Units For Time-Stamping of External Events
- On-Chip Position Encoder Interface Circuitry
- Applicable for Multiple Motor and Converter Control
- 10-Bit Analog-to-Digital Converter (ADC)
 - 8 or 16 Multiplexed Input Channels
 - 500 ns Minimum Conversion Time
 - Selectable Twin 8-Input Sequencers Triggered by Two Event Managers
- 40 Individually Programmable, Multiplexed General-Purpose Input/Output (GPIO) Pins

The control board has the function of rendering the control law. The linear and angular velocities which are derived from the control law, then, control of the servo control modules.

With the functions on TMS320LF2407 above, the controller and user interface were designed and their schematic diagram are shown in Fig. 3-11.

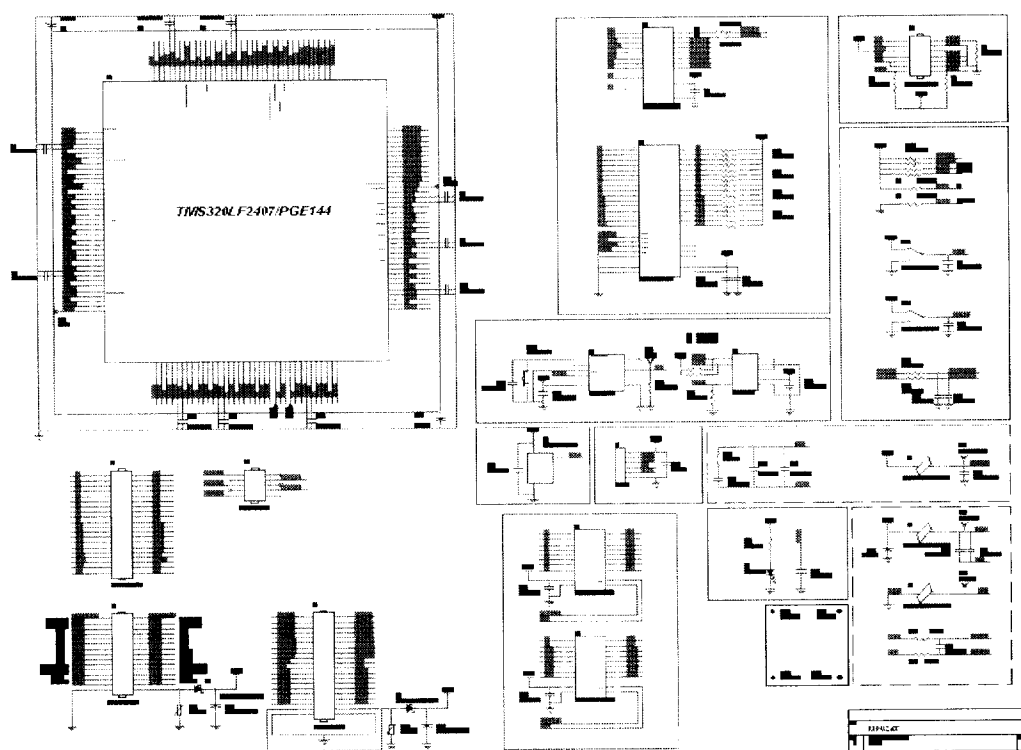


Fig.3-11 Schematic diagram of the controller using TMS320LF2407

Chapter 4

Simulation and Experimental Results

To verify the effectiveness of the proposed controller, simulations and experiments have been done for a mobile manipulator to tracking welding line. The controller is used for the simulation: *full-state feedback controller*. In the simulation, two kinds of welding line are considered for the mobile robot as the following: straight line with $\phi_r(0) = 30^\circ$ and curve line with the radius of 150mm. The mobile manipulator parameters are $b=105mm$, $r=25mm$, $l_1=250mm$, $l_2=250mm$, $l_3=250mm$, $l_4=10mm$ and $l_5=250mm$. The desired linear velocity of the mobile robot is $v=100mm/s$. The experimental mobile robot for straight line and curve line is shown in Photo. 4.1 and Photo. 4.2, respectively.

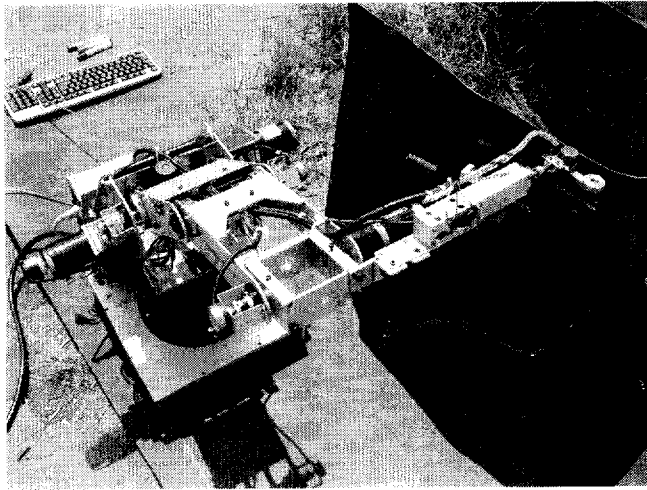


Photo 4.1 experimental mobile robot tracking straight line

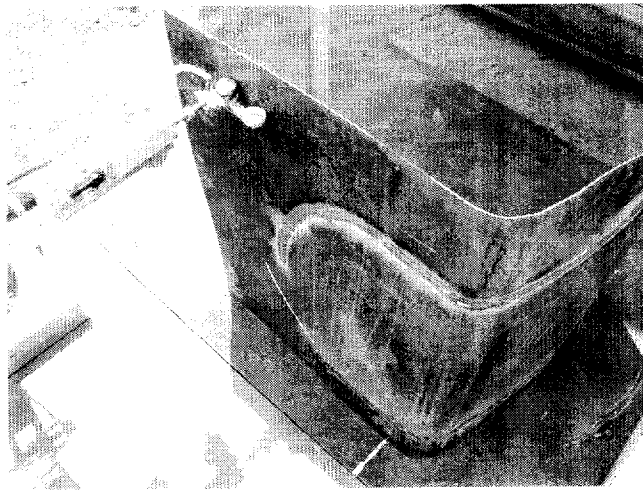


Photo 4.2 experimental mobile robot tracking curve line

4.1 Case of straight Line

The controller (2.20) is used. Table 4-1 shows the initial values and control values for the mobile manipulator system used in this simulation. The simulation results for the straight welding line are shown through Figs. 4-1~4-6.

Table 4-1 Iitial values for simulation

Parameters	Values	Units	Parameters	Values	Units
K_1	3	-	$\Phi_R - \Phi_E (t=0)$	15	deg.
K_2	100	-	$v_E (t=0)$	0	m/s
K_3	5	-	$\omega_E (t=0)$	0	rad/s
K_4	3	-	$\theta_1 (t=0)$	0	deg.
v_R	0.1	m/s	$\theta_2 (t=0)$	30	deg.
$\omega_R (t=0)$	0	rad/s	$\theta_3 (t=0)$	30	deg.
$X_R - X_E(t=0)$	0.005	m	$\theta_4 (t=0)$	30	deg.
$Y_R - Y_E(t=0)$	0.005	m			

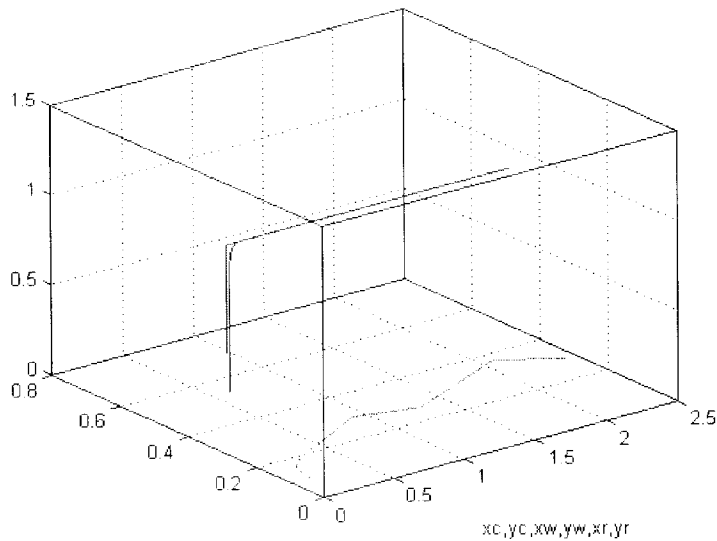


Fig. 4-1 Configuration of the mobile manipulator tracking along the welding path

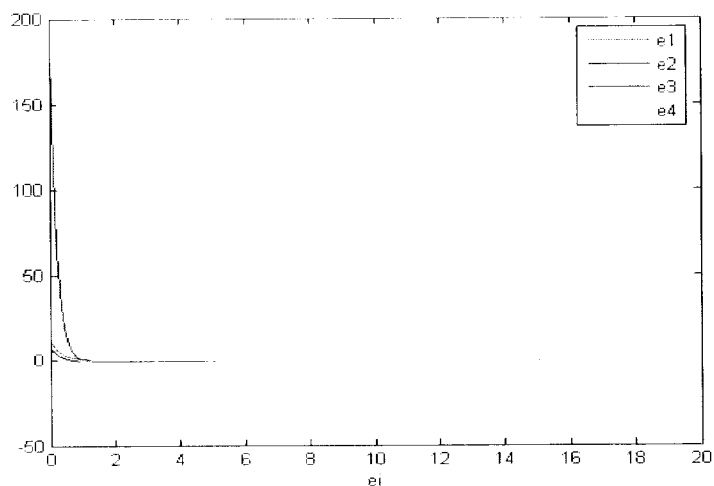


Fig. 4-2 Tracking errors e_1, e_2, e_3, e_4

Fig. 4-1 shows that the end effector of manipulator tracks to the welding point on the reference trajectory. Fig. 4-2 shows the tracking errors of the end effector in whole welding process.

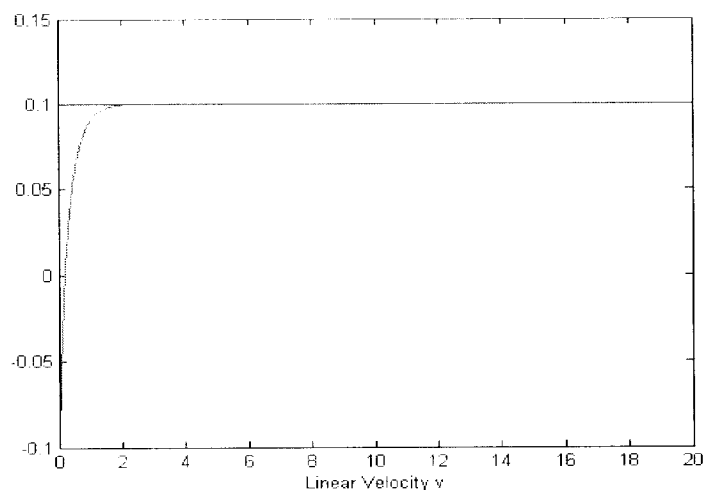


Fig. 4-3 Velocities of the welding reference point and the end effector

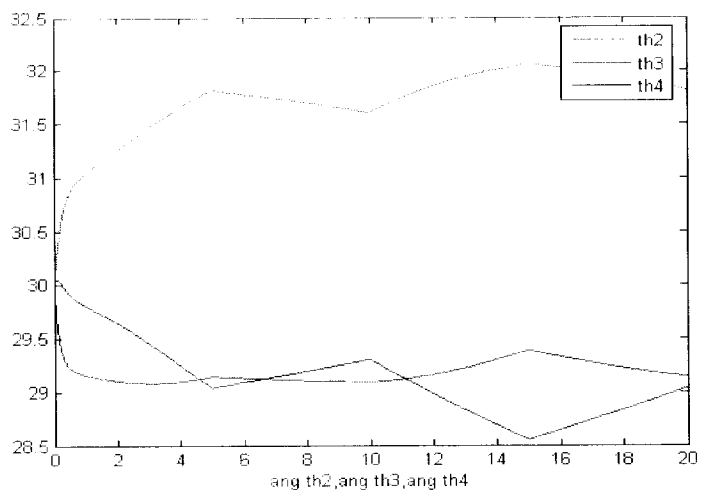


Fig. 4-4 Angle values of three revolute joints

Fig. 4-3 shows the linear velocities of the end effector. Fig. 4-4 shows the angle values of three joints.

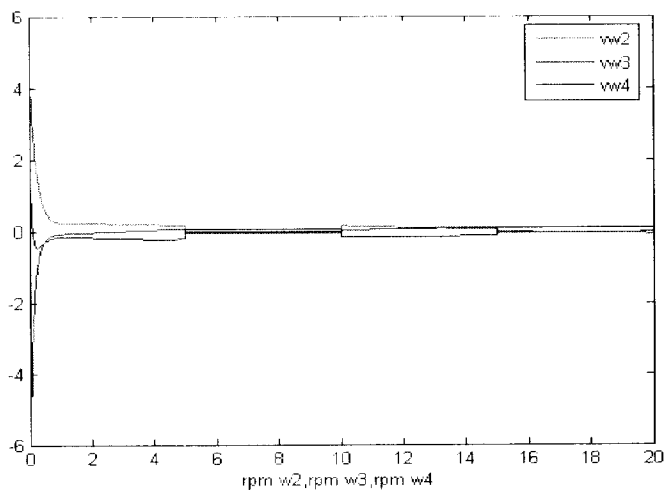


Fig. 4-5 Angular velocities of three revolute joints of the manipulator

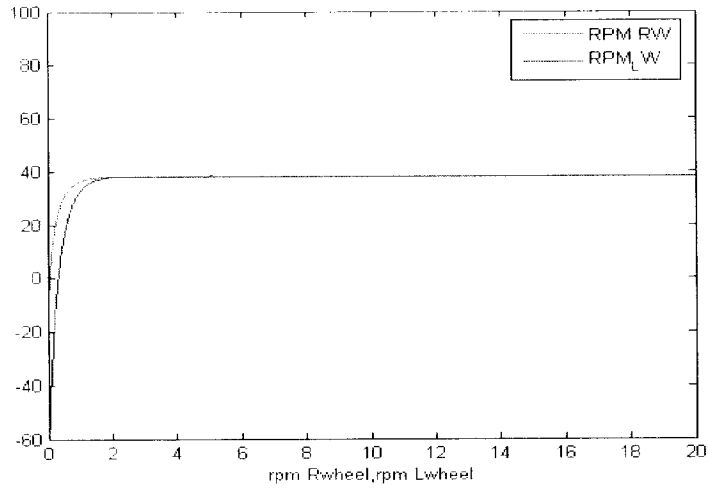


Fig. 4-6 Angular velocities of two wheels of the mobile platform

The angular velocities of three joints in whole the welding process are shown in Fig. 4-5. Fig. 4-6 shows the angular velocities of left and right wheels of the mobile platform.

4.2 Case of Curve line

Table 4-1 shows the initial values and control values for the mobile manipulator system used in this simulation. The simulation results for the curve welding line are shown through Figs. 4-7~4-12.

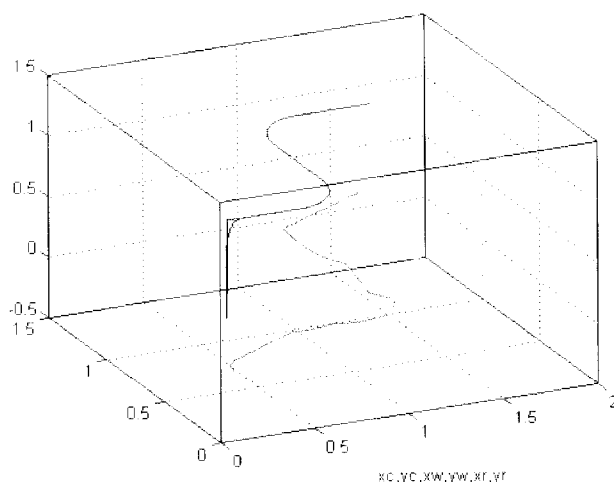


Fig. 4-7 Configuration of the mobile manipulator tracking along the welding path

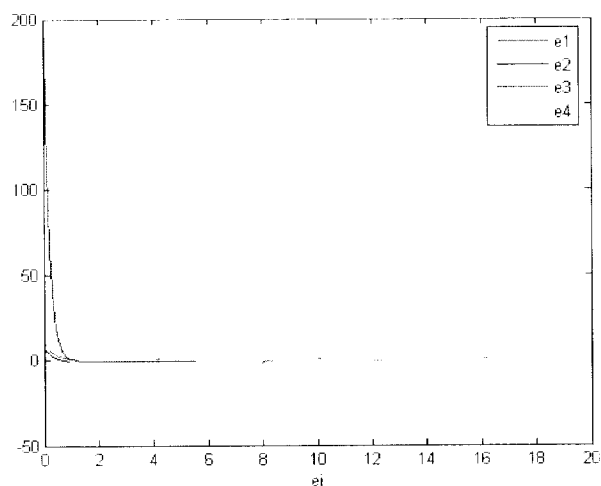


Fig. 5-8 Tracking errors e_1, e_2, e_3, e_4

Fig. 4-7 shows that the end effector of manipulator tracks to the welding point on the reference trajectory. Fig. 4-8 shows the tracking errors of the end effector in whole welding process.

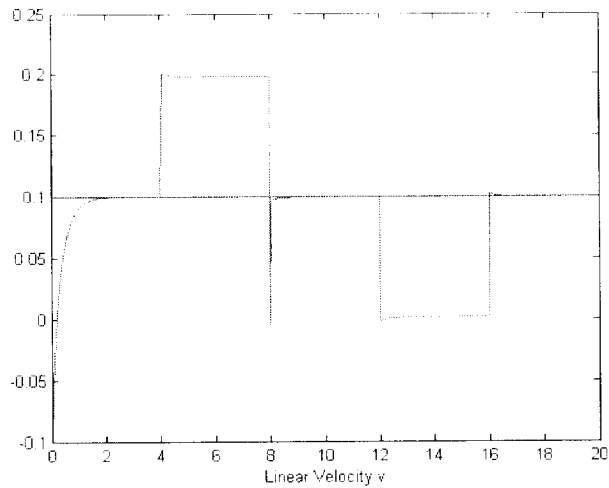


Fig. 4-9 Velocities of the welding reference point and the end effector

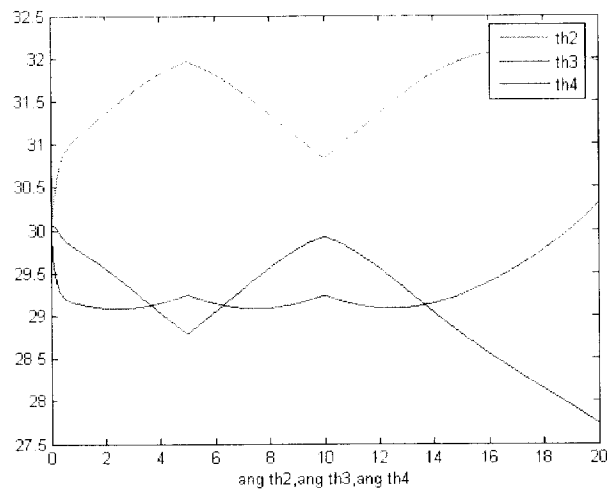


Fig. 4-10 Angle values of three revolute joints

Fig. 4-9 shows the linear velocities of the end effector. Fig. 5-10 shows the angle values of three joints.

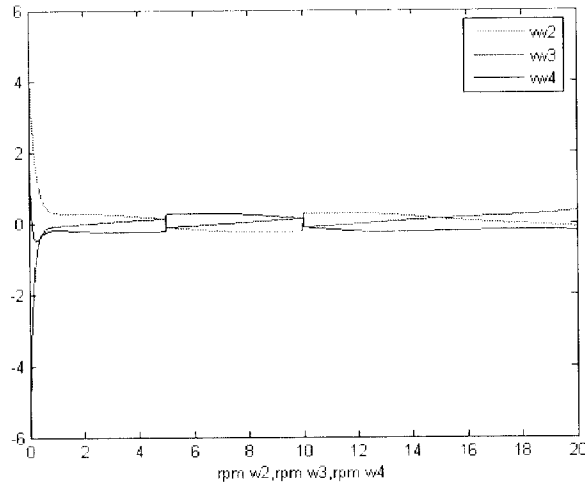


Fig. 4-11 Angular velocities of three revolute joints of the manipulator

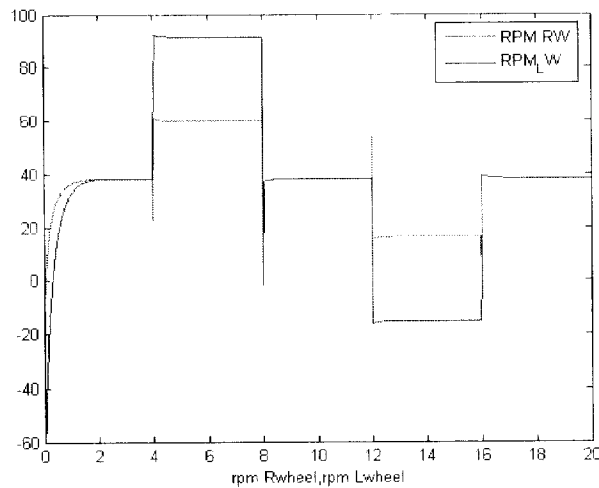


Fig. 4-12 Angular velocities of two wheels of the mobile platform

The angular velocities of three joints in whole the welding process are shown in Fig. 4-11. Fig. 4-12 shows the angular velocities of left and right wheels of the mobile platform.

4.2 Experimental Results

A mobile manipulator prototype has constructed to verify the simulation results on computer. Five DC motors (15W/24V) are used to drive three revolute joints and two wheels. Each DC motor has an encoder to measure its angular velocity, and each revolute joint has a rotary potentiometer to measure its joint angle values. The parameters of the mobile manipulator and the initial parameters are same to in the simulation.

In experiment, when the mobile manipulator tracks along a smooth curved path, the end effector moves along the welding trajectory with a constant inclining angle and constant velocity and then the mobile platform moves to maintain the initial configuration of the manipulator at the same time. This proves that the proposed controllers can control the mobile manipulator to perform the welding process.

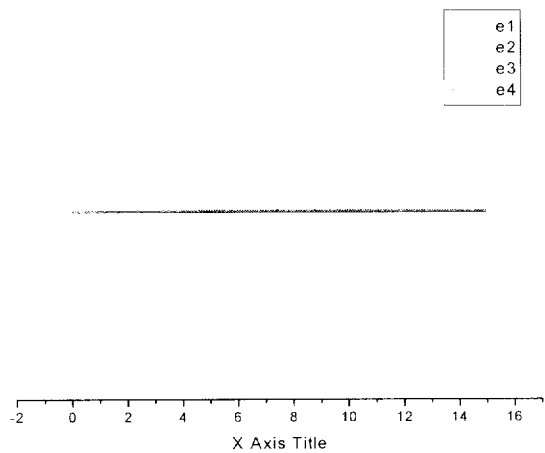


Fig. 4-13 Tracking error from the experiment

Form the experiment result (Fig. 4-13), it is shown that the tracking errors vibrate around zero. These vibrations occur from several causes such as the backlash of the gear. These vibrations occur from several causes such as the backlash of the gear, the rough of the steel wall, disturbances from the electronic circuit and so on.

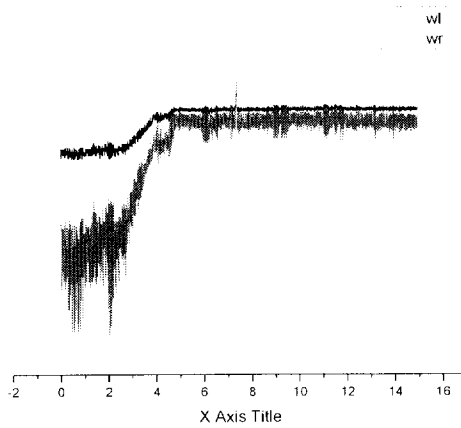


Fig. 4-14 Left and right wheel angular velocities

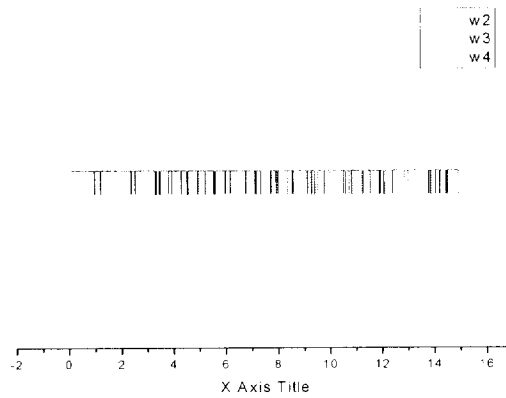


Fig. 4-15 Angular velocities of three revolute joints of the manipulator

Fig. 4-14 shows the angular velocities of three joints of the manipulator. Fig.4-15 shows the left and right wheel angular velocities of mobile robot.

Chapter 5

Conclusions and Future Work

5.1 Conclusions

In this thesis, a simple nonlinear feedback control algorithm based on the kinematic model of a mobile manipulator is proposed for mobile manipulator traveling over irregular terrain. Even if the controller is very simple and easy for applying, it also shows the ability to make a good performance for the mobile manipulator in tracking duty. The uniform asymptotical stability of the system is guaranteed by Lyapunov - like analysis using Barbalat's lemma. It also proves that at the equilibrium point, the tracking errors simultaneously equal to zero. The affirmation in terms of the theory is made out by the simulation step and the experiment step is performed for confirming the feasibility of algorithm in actual welding process.

The contribution in this chapter:

- ❖ Establishing a nonlinear feedback controller based on the kinematic model for a mobile manipulator performing the welding trajectory.

- ❖ Specifying a set of weight factors used in this mobile manipulator's controller for satisfying the rate of initial deviation: 0-20mm with position error and 0-0.3rad with orientation error.

5.2 The Future Work

This thesis described a study on one among the problems of mobile manipulator: Motion control of mobile manipulator moving on irregular terrain. This is the first step in the development of indoor navigate mobile manipulator in the future; that is to say, several other operations such as task planning, path planning, obstacle avoidance, environmental map building can be used and sensor fusion, such as camera, laser sensor, ultrasonic sensor, can be applied to make the mobile manipulator more intelligent in that sense. Therefore, it would be considered as future work the following problems.

5.2.1 Mobile Manipulator Modeling

In this thesis, the kinematics of mobile manipulator model is studied. For most of cases the kinematic model is still applicable in the case of indoor environment. But, dynamics model is always needed when doing research on mobile manipulators to give the best performance that take into account the mass of the mobile manipulator.

5.2.2 Design of the controller

Considering to the other kinds of adaptive control and robust control, continuously try to apply the new algorithms to find out the adequate one for introducing to the mobile manipulator. And concentrating to the hybrid algorithms established by the adaptive control and the robust control so can make the new

controller with the higher flexibility.

References

- [1] Tr. H. Bui, T. T. Nguyen, T. L. Chung, and S. B. Kim, "A Simple Nonlinear Control of a Two-Wheeled Welding Mobile Robot", *Transactions on International Journal of Control, Automation, and Systems (IJCAS)*, Vol. 1, No. 1, pp. 35-42, 2003.
- [2] J. J. Craig, P. Hsu, and S. S. Sastry, "Adaptive Control of Mechanical Manipulators", *Proceedings of the IEEE International Conference on Robotics and Automation*, Vol. 2, pp. 190-195, 1986.
- [3] M. P. Cheng, and C. C. Tsai, "Dynamic Modeling and Tracking Control of a Nonholonomic Wheeled Mobile Manipulator with Two Robotic Arms", *Proceedings of the IEEE Conference on Decision and Control*, Vol. 3, pp. 2932-2937, 2003.
- [4] M. Tarokh, "A Decentralized Nonlinear Three-Term Controller for Manipulator Trajectory Tracking", *Proceedings of the IEEE International Conference on Robotics and Automation*, Minnesota, pp. 3683-3688, April 1996.
- [5] R. Colbaugh, H. Seraji, and K. Glass, "A New Approach to Adaptive Manipulator Control", *Proceedings of the IEEE International Conference on Robotics and Automation*, Vol. 1, pp. 604-611, May 1993.
- [6] B. d'Andrea-Novet, G. Bastin, and G. Campion, "Modeling and Control of Non-holonomic Wheeled Mobile Robots", *Proceedings of the IEEE International Conference on Robotics and Automation*, California, pp.

1130-1135, April 1991.

- [7] C. Abdallah, D. M. Dawson, P. Dorato, and M. Jamshidi, "Survey of Robust Control for Rigid Robots", *IEEE Transactions on Control Systems Magazine*, Vol. 11, pp. 24-30, 1991.
- [8] W. Dong, and W. L. Xu, "Adaptive Tracking of Uncertain Nonholonomic Dynamic System", *IEEE Transactions on Automatic Control*, Vol. 46, No. 3, pp. 450-454, March 2001.
- [9] B. Bayle, I. Y. Fourquet, F. Lamiraux, and M. Renaud, "Kinematic Control of Wheeled Mobile Manipulators", *Proceedings of the IEEE/RSJ International Conference on Intelligent Robots and Systems*, Vol. 2, pp. 1572-1577, 2002.
- [10] B. O. Kam, Y. B. Jeon, and S. B. Kim. "Motion Control of Two-Wheeled Welding Mobile Robot with Seam Tracking Sensor", *Proceedings of the IEEE International Conference Symposium on Industrial Electronics*, Vol. 2, pp. 851-856, June 2001.
- [11] H. Wang, T. Fukao, and N. Adachi, "An Adaptive Tracking Control Approach for Nonholonomic Mobile Robot", *Proceedings of the IFAC World Congress*, pp. 609-615, 1999.
- [12] R. Fierro, and F. L. Lewis, "Control of a Nonholonomic Mobile Robot Using Neural Networks", *IEEE Transactions on Neural Networks*, Vol. 9, No. 4, pp. 589-600, 1998.
- [13] W. Dong, Y. Xu, and Q. Wang, "On Tracking Control of Mobile Manipulators", *Proceedings of the IEEE International Conference on Robotics and Automation*, Vol. 4, pp. 3455-3460, 2000.

- [14] Mamoru Mianami, Masatoshi Hatano, Toshiyuki Asakura : A study of Mobile Manipulators Traveling On Irregular Terrain (1st Report. Derivation of Constrained Dynamic Model and Simulation), Transactions of the Japan Society of Mechanical Engineers, 63-615 C(1997), 3961-3968
- [15] Masatoshi Hatano, Mamoru Minami, Tsuyoshi Ohsumi and Haruki Obara, Modeling of Mobile Manipulators on irregular terrain and Evaluation of Disturbance Torques Department of Mechatronic Engineering, Proceeding of the IEEE/ASME International Conference on Advanced Intelligent Mechatronics, Italy, 2001.
- [16] K. Iagnemma, and S. Dubowsky, Vehicle Wheel-Ground Contact Angle Estimation with Application to Mobile Robot Traction Control, 7th International Symposium on Advances in Robot Kinematics, ARK '00, pp. 137-146, 200.
- [17] F. L. Lewis, C. T. Abdallah and D. M. Dawson, *Control of Robot Manipulators*, Macmillan Publishing Company, New York, USA, 1993.
- [18] J. J. E. Soltine and W. Li, *Applied Nonlinear Control*, Prentice Hall International, 1991.
- [19] K. J. Astrom and B. Wittenmark, *Adaptive Control*, Addison Wesley Publishing Company, 1995.
- [20] N. A. N. Hootsmans, *The Motion Control of Manipulators on Mobile Vehicles*, Ph. D. Thesis, Department of Mechanical Engineering, Massachusetts Institute of Technology, USA, 1992.

Publications and Conferences

A. Publications

- [1] Seung-Mok Shin, Jin-Ho Suh, Jae-Sung Im, Hui-Ryong Yoo, Sang-Bong Kim, "Development of Third-Party Damage Monitoring System for Natural Gas Pipeline," KSME International Journal. Vol.17, No.10, pp1423~1430, 2003.
- [2] Seung Min Kim, Jin Ho Suh, Jae Sung Im, Seong Bong Kim and Sang Bong Kim, "A Smart Memory Type of Data Acquisition System for Shaft Misalignment Maintenance,," Journal of Mechanical Science and Technology Vol.19, No.1, pp. 15-28, 2005.

B. Proceedings and Conferences

- [1] S.M. Shin, H.R. Yoo, J.S. Im, and S.B. Kim, "Development of Third-Party Damage Monitoring System for Natural Gas Pipeline", Proceedings of the 8th Conference on Science and Technology, Control & Automation, pp.119-124, Vietnam National University, HCM City, April, 2002.
- [2] Jae sung Im, Seung Min Kim, Seung Bong Kim, and Sang Bong Kim "A Smart Memory Type of Data Acquisition System for Shaft Misalignment Maintenance" 「The 2003 IntionalInternal Symposium on Mechatronics」

pp16-20 ,Vietnam National University, HCM City, September, 2003.

- [3] Seung Min Kim, Jae Sung Im, Seung Bong Kim, and Sang Bong Kim, "Characteristic of a Turbine Shaft Alignment Using Strain Gauge Data Acquisition System" 「 The 2003 IntionalInternal Symposium on Mechatronics 」 pp46-53 ,Vietnam National University, HCM City, September, 2003.
- [4] Jae Sung Im, Seung Min Kim, Seong Bong Kim and Sang Bong Kim, "Development of Smart Memory Device for Data Acquisition to Shaft Misalignment Maintnace" 「 Proceedings of The 2003 International Symposium on Advanced Engineering 」 pp432-436, Pukyong National University, Busan, Korea 2003.11.13-15.
- [5] Tan Lam Chung, Jae Sung Im, Trong Hieu Bui, and Sang Bong Kim, "Control of Dynamic Mobile Robot for Path Tracking using USB Camera" 「 Proceedings of The 2003 International Symposium on Advanced Engineering 」 pp415-420, Pukyong National University, Busan, Korea 2003.11.13-15.
- [6] Manh Dung Ngo, Jae Sung Im, Hak kyong Kim, and Sang Bong Kim, "Nonlinear Adaptive Sliding Mode Control of Nonhololomic Two-Weeled Welding Mobile Robot for Tracking a Smooth Curved Path" 2003 제어.자동화.시스템 공학회 합동학술발표대회 논문집, pp276-282, 2003.12.12-13